

Peripheral, Non-Centrosome-Associated Microtubules Contribute to Spindle Formation in Centrosome-Containing Cells

U.S. Tulu, N.M. Rusan, and P. Wadsworth*

Department of Biology and
Program in Molecular and Cellular Biology
University of Massachusetts
Amherst, Massachusetts 01003

Summary

In centrosome-containing cells, microtubules utilized in spindle formation are thought to be nucleated at the centrosome. However, spindle formation can proceed following experimental destruction of centrosomes [1] or in cells lacking centrosomes [2], suggesting that non-centrosome-associated microtubules may contribute to spindle formation, at least when centrosomes are absent. Direct observation of prometaphase cells expressing GFP- α -tubulin shows that peripheral, non-centrosome-associated microtubules are utilized in spindle formation, even in the presence of centrosomes. Clusters of peripheral microtubules moved into the centrosomal region, demonstrating that a centrosomal microtubule array can be composed of both centrosomally nucleated and peripheral microtubules. Peripheral bundles also moved laterally into the forming spindle between the spindle poles; 3D reconstructions of fixed cells reveal interactions between peripheral and centrosome-associated microtubules. The spindle pole component NuMA and γ -tubulin were present at the foci of peripheral microtubule clusters, indicating that microtubules moved into the spindle with minus ends leading. Photobleach and photoactivation-marking experiments of cells expressing GFP-tubulin or a photoactivatable variant of GFP-tubulin, respectively, demonstrate that microtubule motion into the forming spindle results from transport and sliding interactions, not treadmilling. Our results directly demonstrate that non-centrosome-associated microtubules contribute to spindle formation in centrosome-containing cells.

Results and Discussion

Peripheral Microtubules Contribute to Spindle Formation

At the entry into mitosis, peripheral non-centrosome-associated microtubules form bundles and clusters that are moved to the region of the forming spindle in a dynein-dependent fashion [3]. Two questions were raised by this earlier work. First, do the peripheral microtubules participate in spindle formation, or are they preferentially disassembled following inward motion? Second, are microtubules transported, or treadmilling, during inward motion (Figure 1A, pathway 1 and 2)?

To determine if peripheral microtubules contribute to spindle formation, we imaged GFP-tubulin expressing LLCPK1 α cells [4] from nuclear envelope breakdown

until late prometaphase when a bipolar spindle was present. The results demonstrate that peripheral bundles and clusters are incorporated into the forming spindle in two ways. In some cases, clusters of peripheral microtubules moved inward along astral microtubules; this is referred to as end-on incorporation (Figure 2A; see Movie 1 in the Supplemental Data). In other cases, microtubule bundles were drawn into the forming spindle in the region between the centrosomes; this is referred to as lateral incorporation (Figure 2B; see Movie 2). In some cases, elements of both processes were evident, and bundles, not focused clusters, were drawn into the aster (see Movie 3).

To demonstrate that the peripheral microtubules moved into the middle of the centrosome, we made photobleach marks (see Experimental Procedures) in front of moving clusters of microtubules. In the example shown in Figure 2C (see Movie 4), a disorganized group of microtubules located at the periphery of the aster reorganizes into a cluster, with a clearly defined focus, and begins inward motion (see Figure 1A, pathway 2). The cluster moves into a bleached region placed in front of the moving microtubules (Figure 2C'), demonstrating that motion continues into the central region of the aster (see Movie 5). These experiments show that a centrosomal microtubule array can be composed of microtubules nucleated at the centrosome as well as non-centrosome-associated microtubules.

To gain insight into the organization of microtubules in prometaphase cells, Z-series of images of fixed cells were collected and deconvolved. The resulting 3D reconstructions showed numerous interactions between extending centrosomal microtubules and microtubules undergoing lateral or end-on incorporation into the forming spindle (Figure 3).

Molecular Composition of Clusters and Bundles

We used immunocytochemistry to determine if centrosome and/or spindle pole components localized to the clusters and bundles of peripheral microtubules. NuMA, which is required for spindle pole formation and localizes to microtubule minus ends at spindle poles [5, 6], was present at the focus of clusters and dispersed along the length of the clustered/bundled microtubules (Figure 4, bottom). γ -tubulin staining was enriched at each centrosome, and in individual planes from a Z-series of images, γ -tubulin staining was also detected both in the spindle and at the focus of microtubule clusters near the centrosome (Figure 4, top) [7]. In contrast, the centrosomal protein pericentrin was clearly present at each centrosome (Figure 4, middle) but was not detected on peripheral microtubule clusters and bundles [8, 9]. The location of NuMA and γ -tubulin indicates that microtubule minus ends are concentrated at the foci of microtubule clusters during inward motion.

Transport and Sliding of Peripheral Microtubules during Inward Motion

Previous observations showed that inward movement of microtubule bundles and clusters requires cytoplasmic

*Correspondence: patw@bio.umass.edu

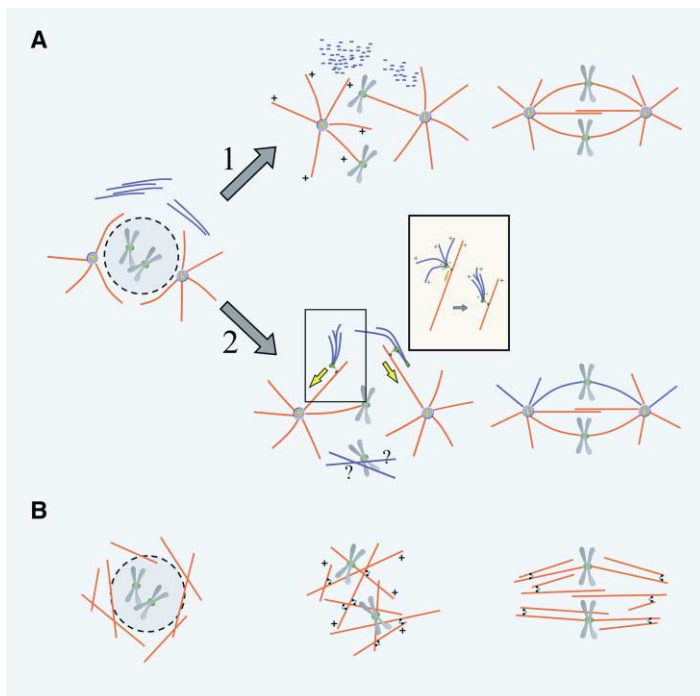


Figure 1. Models for Microtubule Behavior during Spindle Formation

(A) Peripheral microtubules (blue) are moved to the region of the forming spindle where they could be depolymerized (1) or utilized in spindle formation (2). In pathway 1, or search and capture, the resulting spindle is composed exclusively of microtubules nucleated at the centrosome. In pathway 2, or search and transport, the spindle is composed of both centrosomal (red) and peripheral (blue) microtubules; arrows indicate transport. The contribution of chromosome-associated microtubules has not been determined. Inset shows the sorting of a radial array of microtubules into a focused cluster.

(B) Chromosome-directed spindle formation; microtubules are assembled in the vicinity of chromatin and transported into a bipolar spindle.

dynein activity, and we proposed that inward motion is mediated by transport and sliding of adjacent microtubules [3], not treadmilling [10]. To test this hypothesis, photobleach marks were placed on microtubule bundles during inward motion. As shown in Figures 5A and 5B (see Movie 6), bleached zones on microtubule bundles are observed to recover fluorescence as microtubules in the bundle move across the bleached region, toward the forming spindle. These data suggest that the microtubules are transported, but it is difficult to follow individual microtubules because dynamic astral microtubules extend into the bleach zone. We estimated a half-time for recovery of photobleached regions on microtubule clusters of 21 ± 10 s ($n = 3$). This value is similar to previous measurements of fluorescence recovery in mitotic spindles [11, 12] and demonstrates that inward-moving microtubule clusters and bundles are highly dynamic.

Because photobleached marks were difficult to detect in regions of high microtubule density, we used photoactivation of fluorescence, which has better signal-to-noise characteristics than photobleaching, to mark microtubules [13]. α -tubulin was tagged with a photoactivatable variant of GFP [14] and expressed in LLCPK1 cells (see Experimental Procedures). The results of photoactivation experiments on prometaphase cells show that microtubules move into the forming spindle along linear or curvilinear paths (Figure 5C; Movie 7) and clearly demonstrate that peripheral microtubules are transported, not treadmilling, during spindle formation.

Do inward-moving microtubules slide relative to other stationary microtubules during inward motion or are they moved by motors tethered to stationary elements of the cell, for example, a spindle matrix [15]? In areas of GFP-tubulin-expressing cells where microtubule density was low, motion of one microtubule relative to another static microtubule was observed (Figure 5D). Evidence for mi-

cro-tubule-microtubule sliding interactions was also obtained from photoactivation experiments. Figure 5E shows a photoactivated region on a microtubule bundle that extends to several times its original length, remarkably similar to the telescoping of axonemal microtubules driven by dynein [16]. In this case, sliding did not occur on an anchored microtubule; therefore, the result was bidirectional elongation, not inward translocation (Figure 5E; Movie 8). These observations support the view that microtubule-microtubule sliding drives transport into the forming spindle. Dynein antibodies have been shown to block clearance of peripheral microtubules [3] and the motion of microtubule fragments on *Xenopus* extract spindles [17]; therefore, sliding of adjacent microtubules in the forming mammalian spindle is also likely to be dynein dependent.

Photoactivation experiments further demonstrated that microtubules undergo periods of motion away from the pole (Figure 5F). Outward movements were infrequent, and the majority of motion is directed inward in prometaphase cells. The observation that microtubules can move bidirectionally indicates that microtubule transport may result from the regulated activity of antagonistic motors. Outward motion was not detected previously because these motions are difficult to detect when all the microtubules are uniformly fluorescent. Microtubules that moved away from the spindle pole almost always disassembled (Figure 5F) as do peripheral microtubules that never began inward motion (data not shown). These data are consistent with the idea that a gradient of activity of spindle assembly factors exists in mitotic cytoplasm [18, 19].

The average rate of inward motion of photoactivated marks on microtubules was 6.8 ± 4.1 $\mu\text{m}/\text{min}$ ($n = 48$), similar to previous estimates of inward motion with GFP-tubulin [3] and to the rate of dynein-dependent motion of microtubule seeds on microtubules in *Xenopus* extracts

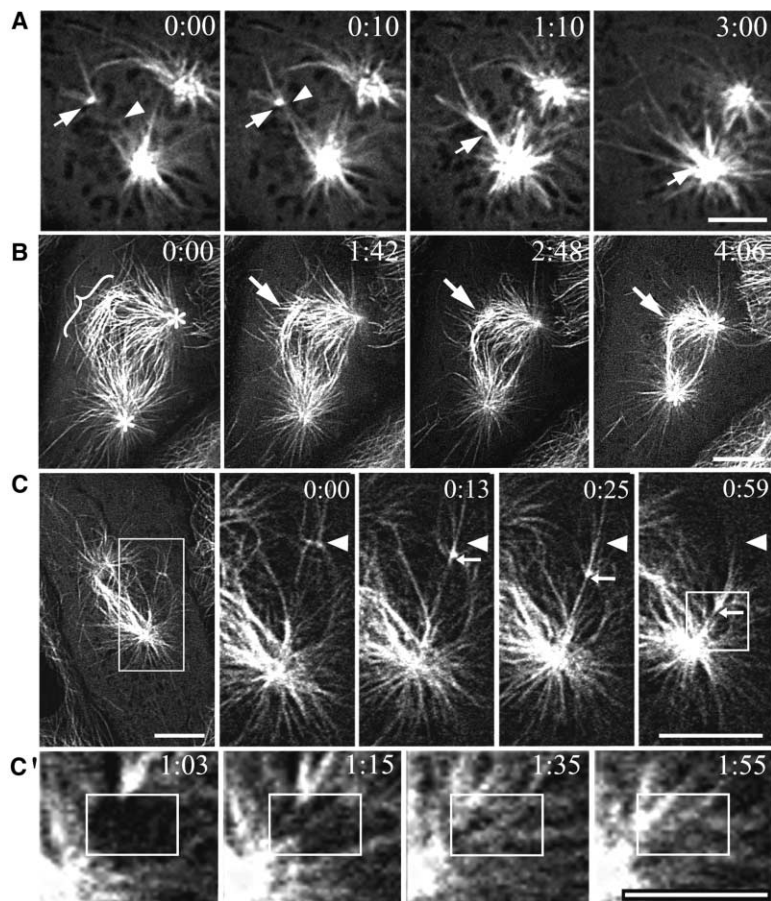


Figure 2. Peripheral Microtubules Contribute to Spindle Formation

Spinning disc (A and B) and laser scanning (C and C') confocal microscopy of LLCPK1 α cells expressing GFP- α -tubulin.

(A) End-on incorporation showing a cluster of microtubules (arrow) that is captured by extending centrosomal microtubules (arrowhead) and drawn into the centrosomal microtubule array.

(B) Lateral incorporation of a peripheral bundle (bracket) into the forming spindle; asterisks mark the centrosomes.

(C) Formation and inward motion of a microtubule cluster; arrowhead marks a constant location, and arrow marks the microtubule cluster.

(C') Enlargement of boxed region in (C). A photobleached mark (box in [C']) was placed in front of the moving cluster; the cluster moves into the bleached zone.

Time in min:s in upper right of each panel. Scale bars, 10 μ m in (A)–(C) and 5 μ m in (C').

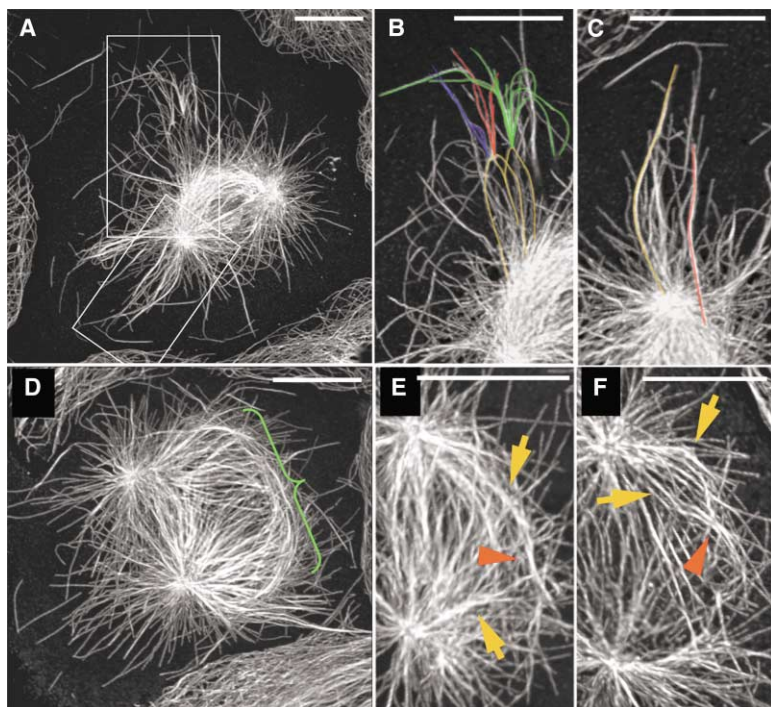


Figure 3. Maximum Intensity Projections of Deconvolved Z-Series of Fixed Cells Stained with Antibodies to Tubulin

Z-series were deconvolved with AutoQuant Software. (A) Microtubule clusters in a prometaphase cell; the boxed regions are enlarged in (B) and (C) and the clusters pseudocolored to aid visualization.

Extending microtubules are frequently curved or looped. (D–F) Three different examples of lateral interactions of peripheral microtubules with the forming spindle; arrows show extending centrosomal microtubules and arrowheads show peripheral, non-centrosome-associated microtubule bundles. Scale bars, 10 μ m.

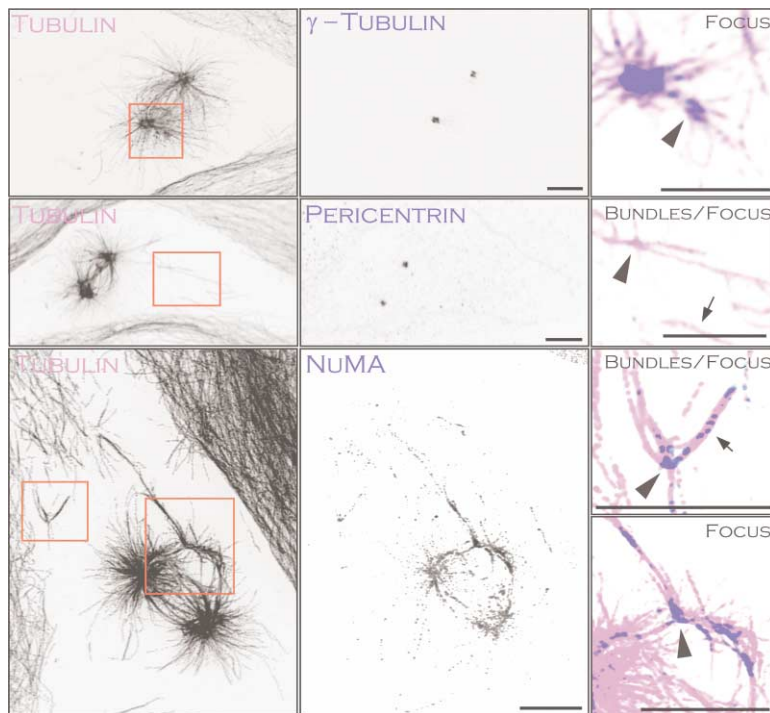


Figure 4. Composition of Microtubule Bundles and Clusters

Immunolocalization of spindle pole and centrosome components in fixed LLCPK1 cells. Left column shows tubulin staining; middle column shows γ -tubulin, pericentrin, and NuMA (top to bottom); and right column shows an overlay of the boxed region; microtubules are violet, pole and centrosome components are in blue. Scale bars, 10 μ m.

[2]. The rate of outward motion was $8.1 \pm 4.9 \mu\text{m}/\text{min}$ ($n = 11$). Measurements of instantaneous velocities showed that individual photoactivated zones moved at highly variable rates (data not shown).

A Model for Spindle Formation in Centrosome-Containing Cells

Our previous observations indicated that peripheral microtubules moved toward the spindle region, but the fate of these microtubules was not determined. One possibility is that peripheral microtubules, which have two free ends, are disassembled in the spindle region (Figure 1A, pathway 1). An alternative possibility, and the one that we observe, is that peripheral microtubules are utilized in the forming spindle (Figure 1A, pathway 2). Heretofore, it has been generally accepted that spindle assembly in centrosome-containing cells occurs by a process known as search and capture [20] in which centrosomally nucleated microtubules search for and capture kinetochores [21] resulting in bipolar spindle formation. However, recent work demonstrates that spindle formation can proceed following experimental removal or destruction of centrosomes [1, 22]. Our observations of spindle assembly in mammalian cells consistently reveal that peripheral, non-centrosome-associated microtubules are transported to, and within, the forming spindle (Figure 1A, pathway 2). Thus, the conventional view that spindle microtubules are solely generated by nucleation at the centrosome (Figure 1A, pathway 1) is inaccurate, at least for mammalian epithelial cells.

Transport of non-centrosome-associated microtubules also occurs during spindle formation in cells lack-

ing centrosomes (Figure 1B). In these cells, noncentrosomal microtubules are assembled in the vicinity of chromatin [23] by a RanGTPase-dependent pathway [24] and are polarity sorted and transported to form a bipolar spindle [25]. Our results demonstrate that transport of noncentrosomal microtubules occurs even in the presence of the centrosome and that spindle formation in cells containing or lacking centrosomes is more similar than previously recognized [26].

Our unexpected observation that the centrosomal array in a mitotic cell is composed of microtubules nucleated at the centrosome and of peripheral microtubules shows that a centrosome is involved not only in microtubule nucleation but contributes to the overall organization of microtubules in mitotic cytoplasm [27, 28]. Although our observations are limited to nonkinetochore microtubules, recent work has shown that kinetochore fibers can form from the distal kinetochore in monastrol-treated cells and that these fibers are subsequently drawn into the centrosome region by minus end-directed motion along extending centrosomal microtubules [30]. Thus, for both nonkinetochore microtubules and kinetochore microtubules, sliding interactions between microtubules of the same polarity contribute to spindle formation. Our data demonstrate that in addition to searching the cytoplasm for kinetochores [29], centrosomal microtubules search for non-centrosome-associated microtubules and serve as tracks for microtubule transport during spindle formation.

Experimental Procedures

Materials

All materials for cell culture were obtained from Invitrogen, with the exceptions of F-10 and antibiotics, which were obtained from

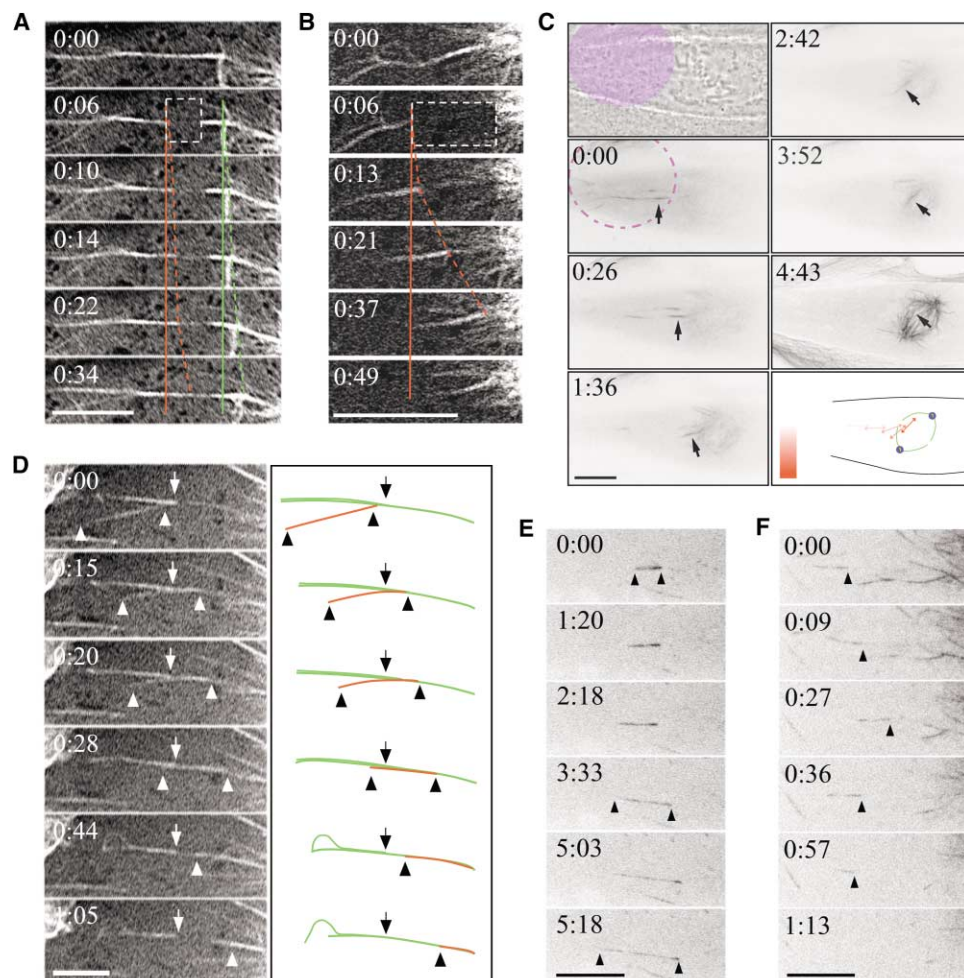


Figure 5. Microtubule Transport and Sliding during Spindle Assembly

The forming spindle is on the right for all images. (A and B) Photobleaching of microtubule bundles during inward motion. Boxes show the bleach, solid red line shows the left edge of the bleached zone, and dotted red line shows fluorescence moving into the bleach zone. In (A), the solid green line marks a constant position and the dotted green line shows the location of a cluster of microtubules. (C) Photoactivation of fluorescence in a cell expressing PA-GFP- α -tubulin. Phase contrast image of the cell at the time of photoactivation (upper left); region of activation is shown as a pink overlay. Contrast has been reversed and photoactivated regions are in dark contrast; time in min:s; arrow marks the position of a photoactivated bundle of microtubules. The whole cell was photoactivated (4:43) to show the entire microtubule array. (Last panel) Schematic diagram of the position of the activated bundle over time, represented by color scale. (D) Microtubule sliding in a cell expressing GFP- α -tubulin; arrowheads mark the ends of a short microtubule; arrow marks a point on a microtubule bundle. (Right panels) Schematic diagram. (E) Elongation of a photoactivated region on a microtubule bundle; arrows mark the ends of the region of photoactivation. (F) Inward and outward motion of a photoactivated region; arrowhead marks the right edge; the photoactivated region eventually disassembles.

Sigma-Aldrich, and fetal bovine serum, which was obtained from Atlanta Biologicals. Unless otherwise noted, all chemicals were obtained from Sigma-Aldrich.

Cell Culture

LLCPK1 α cells were cultured in a 1:1 mixture of Opti-MEM and F-10 media supplemented with 7.5% fetal bovine serum and antibiotics. Cells were grown in a 5% CO₂ atmosphere at 37°C. For use in experiments, cells were either plated on glass coverslips or glass-bottomed dishes (MatTek Corp).

Immunofluorescence Microscopy

The following antibodies were used in these experiments: anti-NuMA, a gift of Dr. D. Compton (Dartmouth Medical School, Hanover, NH), used at 1:5000; anti-pericentrin (Covance) used at 1:100; anti-tubulin, clone YL1/2 (Accurate Chemical), used at 1:2; and anti- γ -tubulin polyclonal (Sigma-Aldrich) used at 1:2000. Cells were fixed in ice-cold methanol, except for the 3D reconstructions, which were

fixed in 1% glutaraldehyde. Incubations with primary antibodies were performed overnight at room temperature or for 1 hr at 37°C; Cy3 (Jackson ImmunoResearch Laboratories) or FITC-labeled secondary antibodies (Sigma-Aldrich) were used at the recommended dilution for 1 hr at room temperature. Coverslips were mounted in Vectashield (Vector Laboratories) and sealed with nail polish.

Image Acquisition

Images were acquired by using a Nikon Eclipse TE 300 microscope equipped with a 100 \times phase, NA 1.4 objective lens, a Perkin Elmer Spinning Disc Confocal Scan head (Perkin Elmer), and a Roper Micromax interline transfer-cooled CCD camera (Roper Scientific). All images were taken with a single wavelength (488 nm) filter cube. Image acquisition was controlled by Metamorph Software (Universal Imaging Corp), and time-lapse sequences were acquired at 2 s intervals with an exposure time of 0.3–0.7 s.

For photoactivation experiments, cells expressing photoactivatable GFP-tagged tubulin were photoactivated by a 5–7 s exposure

to 413 nm light (excitation filter D405/20, Chroma Tech Corp) from a shuttered 100W mercury arc epilluminator. The area of photoactivation was selected by reducing the area of the field diaphragm or by using pinholes and slits (Lenox Laser) mounted in a Ludl filter wheel (Ludl Electronic Products) placed in a conjugate image plane in the light path. Following photoactivation, confocal image acquisition proceeded as described above.

For photobleaching experiments, a Zeiss 510 META confocal scanning system was used. Images were acquired by using a 60 \times , NA 1.4 objective lens. The argon laser was used at 50% power of 30mW. For imaging, averages of four to eight line scans were taken at 4 to 5 s intervals; 5% laser transmission was used. For bleaching, the laser was used at 100% transmission for 70 iterations at 488 nm.

Cloning of PAGFP- α -Tubulin

Human α tubulin from the pEGFP- α -tubulin vector (BD Sciences Clontech) was excised with BamHI and XhoI restriction enzymes and ligated into PAGFP-C1 vector, gift of Drs. G. Patterson and J. Lippincott-Schwartz (National Institute of Child Health and Human Development, Bethesda, MD). The resulting fusion of PAGFP- α -tubulin was then excised with BamHI and NheI restriction enzymes and ligated into the pIRESneo2 vector (BD Sciences Clontech).

Supplemental Data

Supplemental data including movies of the data shown as still images in Figures 2 and 5 are available at <http://www.current-biology.com/cgi/content/full/13/21/1894/DC1>.

Received: August 5, 2003

Revised: September 11, 2003

Accepted: September 12, 2003

Published: October 28, 2003

References

1. Khodjakov, A., Cole, R.W., Oakley, B.R., and Rieder, C.L. (2000). Centrosome-independent mitotic spindle formation in vertebrates. *Curr. Biol.* 10, 59–67.
2. Heald, R., Tournebize, R., Blank, T., Sandaltzopoulos, R., Becker, P., Hyman, A.A., and Karsenti, E. (1996). Self-organization of microtubules into bipolar spindles around artificial chromosomes in *Xenopus* egg extracts. *Nature* 382, 420–425.
3. Rusan, N.M., Tulu, U.S., Fagerstrom, C., and Wadsworth, P. (2002). Microtubule rearrangement in prophase/prometaphase cells requires cytoplasmic dynein. *J. Cell Biol.* 158, 997–1003.
4. Rusan, N.M., Fagerstrom, C., Yvon, A.C., and Wadsworth, P. (2001). Cell cycle-dependent changes in microtubule dynamics in living cells expressing GFP- α tubulin. *Mol. Biol. Cell* 12, 971–980.
5. Compton, D.A. (2000). Spindle assembly in animal cells. *Annu. Rev. Biochem.* 69, 95–114.
6. Merdes, A., Heald, R., Samejima, K., Earnshaw, W.C., and Cleveland, D.W. (2000). Formation of spindle poles by dynein/dynactin-dependent transport of NuMA. *J. Cell Biol.* 149, 851–861.
7. Lajoie-Mazenc, I., Tollon, Y., Detraves, C., Julian, M., Moisand, A., Gueth-Hallonet, C., Debec, A., Salles-Passador, I., Puget, A., Mazarguil, H., et al. (1994). Recruitment of antigenic gamma-tubulin during mitosis in animal cells: presence of gamma-tubulin in the mitotic spindle. *J. Cell Sci.* 107, 2825–2837.
8. Doxsey, S.J. (2001). Centrosomes as command centres of cellular control. *Nat. Cell Biol.* 3, E105–E108.
9. Andersen, S.S.L. (1999). Molecular characteristics of the centrosome. *Int. Rev. Cytol.* 187, 51–109.
10. Rodionov, V.I., and Borisy, G.G. (1997). Microtubule treadmill in vivo. *Science* 275, 215–218.
11. Saxton, W.M., Stemple, D.L., Leslie, R.J., Salmon, E.D., Zavorzink, M., and McIntosh, J.R. (1984). Tubulin dynamics in cultured mammalian cells. *J. Cell Biol.* 99, 2175–2186.
12. Wadsworth, P., and Salmon, E.D. (1986). Microtubule dynamics in mitotic spindles of living cells. In *Dynamic Aspects of Microtubule Biology*, Volume 466, D. Soifer, ed. (New York: The New York Academy of Sciences), pp. 580–592.
13. Mitchison, T.J. (1989). Polewards microtubule flux in the mitotic spindle: evidence from photoactivation of fluorescence. *J. Cell Biol.* 109, 637–652.
14. Patterson, G.H., and Lippincott-Schwartz, J. (2002). A photoactivatable GFP for selective photolabeling of proteins and cells. *Science* 297, 1873–1877.
15. Scholey, J.M., Rogers, G.C., and Sharp, D.J. (2001). Mitosis, microtubules and the matrix. *J. Cell Biol.* 154, 261–266.
16. Summers, K.E., and Gibbons, I.R. (1971). Adenosine triphosphate-induced sliding of tubules in trypsin-treated flagella of sea urchin sperm. *Proc. Natl. Acad. Sci. USA* 68, 3092–3096.
17. Heald, R., Tournebize, R., Habermann, A., Karsenti, E., and Hyman, A. (1997). Spindle assembly in *Xenopus* egg extracts: respective roles of centrosomes and microtubule self-organization. *J. Cell Biol.* 138, 615–628.
18. Kalab, P., Weis, K., and Heald, R. (2002). Visualization of a Ran-GTP gradient in interphase and mitotic *Xenopus* egg extracts. *Science* 295, 2452–2456.
19. Verde, F., Labbe, J.-C., Doree, M., and Karsenti, E. (1990). Regulation of microtubule dynamics by cdc2 protein kinase in cell-free extracts of *Xenopus* eggs. *Nature* 343, 233–237.
20. Kirschner, M.W., and Mitchinson, T. (1986). Beyond self assembly: from microtubule to morphogenesis. *Cell* 45, 329–342.
21. Rieder, C.L., and Alexander, S.P. (1991). Kinetochore are transported poleward along a single astral microtubule during chromosome attachment to the spindle in newt lung cells. *J. Cell Biol.* 110, 81–95.
22. Hinchcliffe, E.H., Cham, M., Khodjakov, A., and Sluder, G. (2001). Requirement of a centrosomal activity for cell cycle progression through G1 into S phase. *Science* 291, 1547–1550.
23. Karsenti, E., Newport, J., Hubble, R., and Kirschner, M.W. (1984). Interconversion of metaphase and interphase microtubule arrays, as studied by the injection of centrosomes and nuclei into *Xenopus* eggs. *J. Cell Biol.* 98, 1730–1745.
24. Walczak, C.E. (2001). Ran hits the ground running. *Nat. Cell Biol.* 3, E69–E71.
25. Heald, R., Tournebize, R., Blank, T., Sandaltzopoulos, R., Becker, P., Hyman, A., and Karsenti, E. (1996). Self-organization of microtubules into bipolar spindles around artificial chromosomes in *Xenopus* egg extracts. *Nature* 382, 420–425.
26. Scholey, J.M., Brust-Mascher, I., and Mogilner, A. (2003). Cell division. *Nature* 422, 746–752.
27. Karsenti, E., and Vernos, I. (2001). The mitotic spindle: a self-made machine. *Science* 294, 543–547.
28. Wittman, T., Hyman, A., and Desai, A. (2001). The spindle: a dynamic assembly of microtubules and motors. *Nat. Cell Biol.* 3, E28–E34.
29. Mitchison, T.J., and Kirschner, M.W. (1984). Microtubule assembly nucleated by isolated centrosomes. *Nature* 312, 232–237.
30. Khodjakov, A., Copenagle, L., Gordon, M.B., Compton, D.A., and Kapoor, T. (2003). Minus-end capture of preformed kinetochore fibers contributes to spindle morphogenesis. *J. Cell Biol.* 160, 671–683.